Vortex motion in Josephson-junction arrays near $f=0$ and $f=1/2$

Wenbin Yu, K. H. Lee, and D. Stroud
Department of Physics, The Ohio State University, Columbus, Ohio 43210
(Received 28 September 1992)

We study vortex motion in two-dimensional Josephson arrays at magnetic fields near zero and one-half flux quanta per plaquette ($f=0$ and $f=\frac{1}{2}$). The array is modeled as a network of resistively and capacitively shunted Josephson junctions at temperature $T=0$. Calculations are carried out over a range of the McCumber-Stewart junction damping parameter β. Near both $f=0$ and $f=\frac{1}{2}$, the I-V characteristics exhibit *two* critical currents, $I_{c1}(f)$ and $I_{c2}(f)$, representing the critical current for depinning a single vortex, and for depinning the entire ground-state phase configuration. Near $f=0$, single vortex motion just above $I_{c1}(0)$ leads to Josephson-like voltage oscillations. The motion of the vortex is seemingly overdamped (i.e., nonhysteretic) even when the individual junction parameters are highly underdamped, in agreement with experiments. At sufficiently large β, and sufficiently high vortex velocity, the vortex breaks up into a row of resistively switched junctions perpendicular to the current. Near $f=\frac{1}{2}$, the vortex potential, and corresponding vortex trajectories, are more complicated than near $f=0$. Nevertheless, the vortex is still "overdamped" even when the individual junctions are highly underdamped, and there is still row-switching behavior at large values of β. A high-energy vortex in a very underdamped array tends to generate resistively switched rows rather than to move ballistically. Some possible explanations for this behavior are discussed.

I. INTRODUCTION

Superconducting arrays are comprised of superconducting (S) grains embedded in a normal (N) or insulating (I) host and linked together by Josephson or proximity effect coupling.[1] Such arrays can be microfabricated with unit cells as small as a few microns on each side in one or two dimensions ($d=1$ or 2) with 1000 or more junctions on a line. They have attracted much interest because they exhibit diverse phase transitions and dynamical properties with and without an applied magnetic field. They also serve as excellent model systems for studying transport in systems, such as high-temperature superconductors, which may contain naturally occurring weak links.

The properties of superconducting arrays are often described in terms of vortices. Such vortices are spatial arrangements of the phase of the superconducting order parameter, which are thought to move through the array as a unit, in response to forces generated, e.g., by currents, magnetic field gradients, or other vortices. Several groups have proposed equations of motion for vortices in arrays. These equations are formally similar to those describing the time dependence of the phase in a single Josephson junction. For example, Rzchowski *et al.*[2] have proposed that a single vortex moving through a homogeneous square lattice of capacitively shunted Josephson junctions satisfies the equation

$$\frac{d^2}{dt^2}\left[2\pi\frac{x}{a}\right]+\frac{1}{RC}\frac{d}{dt}\left[2\pi\frac{x}{a}\right]+\frac{4e}{\hbar C}\left[I_d\sin\left[2\pi\frac{x}{a}\right]-I\right]=0\ , \quad (1)$$

where x is the vortex position along a line through the plaquette centers and perpendicular to the external current I, a is the lattice constant, R and C are the shunt resistance and shunt capacitance of each junction, and I_d is the vortex depinning current.[3]

Although coherent vortex motion is not necessarily excluded from overdamped arrays, such motion may be easier to detect in underdamped systems. Experiments in such arrays have been carried out by several groups.[4-9] These arrays are typically made from small grains in which the charging energy[10] is non-negligible. They are expected to exhibit a variety of phenomena not necessarily found in proximity-coupled arrays, which are usually overdamped[11] and have negligible capacitive charging energies. Several of these experiments[2,4-7] have given unambiguous evidence of vortex motion. Coherent vortex motion is suggested, in particular, by the observation of vortex depinning currents at low temperatures, and of a resistivity proportional to the magnetic field with an activated temperature dependence.[4] Such a resistivity is expected when vortices are thermally excited out of a potential well.[12] In addition, evidence of quantum vortex motion has been reported,[5,6] consistent with expectations for highly underdamped arrays at sufficiently low temperatures.[13-15]

In this paper, we show numerically, starting from the relevant equations of motion for the Josephson phases, that a vortex pattern in either an underdamped or an overdamped Josephson-junction array can behave very much like a coherent particle. In the overdamped limit, the vortex acts as if it moves in a sinusoidal periodic two-dimensional potential,[16,17] exhibiting a time-dependent voltage similar to that of a single Josephson junction. In the underdamped regime, the vortex contin-

ues to behave like a coherent object. However, even in an array of strongly underdamped individual junctions, the vortex is still overdamped in that it produces an I-V characteristic with little hysteresis, in agreement with the experimental observations of Refs. 5 and 6. Hysteretic I-V characteristics may set in at extremely high values of the junction McCumber-Stewart parameter β,[18] which is a measure of the damping. At sufficiently large β, we see evidence for "row switching," in which an entire row of junctions switches into a resistive state. This behavior has been reported in previous calculations[19] and seen in experiments.[4-8]

Consistent with the coherent vortex picture, we find that an ordered array near $f=0$ exhibits, in effect, *two* critical currents, $I_{c1}(0)$ and $I_{c2}(0)$, as suggested previously on the basis of static calculations.[2,3] (f represents the flux per plaquette, measured in unit of a single flux quantum $\Phi_0=hc/2e$.) The lower critical current represents the depinning of individual vortices, while the upper corresponds to the depinning of the entire $f=0$ ground-state phase configuration. When $f=\frac{1}{2}+\delta$, where $|\delta|\ll 1$, we again find two critical currents $I_{c1}(\frac{1}{2})$ and $I_{c2}(\frac{1}{2})$. In this case, $I_{c1}(\frac{1}{2})$ is the current necessary to depin a single vortex from the checkerboard[20] $f=\frac{1}{2}$ ground-state vortex configuration. $I_{c2}(\frac{1}{2})$ is the current required to depin the entire $f=\frac{1}{2}$ ground-state lattice. The time-dependent voltage $V(t)$ just above $I_{c1}(\frac{1}{2})$ is complicated and depends both on β and on the initial phase configuration.

We turn now to the body of the paper. Section II describes our model equations, choice of gauge, and numerical method. Our results are presented in Sec. III, followed by a brief discussion in Sec. IV.

II. FORMALISM

A. Coupled RCSJ model

In the limit of weak screening, a Josephson junction array is well described by the coupled RCSJ model (resistively and capacitively shunted junction model). In this model, the current through a Josephson junction consists of four components: the capacitive charging current, the resistive ohmic current, the Josephson supercurrent, and the thermal noise current. In this paper, all calculations are carried out at zero temperature, so that the thermal noise current does not contribute. The coupled RCSJ equations then take the form[19,21]

$$I_{ij}=C_{ij}\frac{d}{dt}V_{ij}+\frac{V_{ij}}{R_{ij}}+I_{c;ij}\sin(\phi_i-\phi_j-A_{ij})\ , \tag{2}$$

$$V_{ij}\equiv V_i-V_j=\frac{\hbar}{2e}\frac{d}{dt}(\phi_i-\phi_j)\ , \tag{3}$$

$$\sum_j I_{ij}=I_{i;\mathrm{ext}}\ , \tag{4}$$

$$A_{ij}=\frac{2\pi}{\Phi_0}\int_{\mathbf{x}_i}^{\mathbf{x}_j}\mathbf{A}\cdot d\mathbf{l}\ . \tag{5}$$

Here ϕ_i is the phase of the order parameter on grain i; $I_{c;ij}$ is the critical current of the Josephson junction connecting grains i and j; R_{ij} and C_{ij} are the shunt resistance and shunt capacitance for the (ij)th junction, which connects grains i and j; and $\mathbf{x}_i$ is the position of the center of grain i. The first equation constitutes the RCSJ model: the current I_{ij} through the (ij)th junction is expressed as the sum of a capacitive charging current, an ohmic shunt current, and a supercurrent. The second equation is the Josephson relation between the phase difference and voltage difference across the (ij)th junction. The third equation is Kirchhoff's Law, which states that the total current leaving grain i into the various neighboring grains equals the total external current $I_{i;\mathrm{ext}}$ fed into that grain. Finally, Eq. (5) is the extra factor required to keep the phase difference gauge invariant in the presence of a vector potential $\mathbf{A}$. We use boundary conditions such that a uniform current $I_{i;\mathrm{ext}}\equiv I$ is fed into each grain along one edge of an array of $N\times N$ square plaquettes, and extracted from each grain on the opposite edge, with periodic boundary conditions in the transverse directions.

Eqs. (2), (3),and (4) can be combined to give

$$\begin{aligned}\sum_j \tilde{C}_{ij}\frac{d}{dt}V_j&=I_{i;\mathrm{ext}}-\sum_j\frac{V_i-V_j}{R_{ij}}\\&\quad-\sum_j I_{c;ij}\sin(\phi_i-\phi_j-A_{ij})\\&\equiv S_i\ ,\end{aligned} \tag{6}$$

$$\frac{d}{dt}\phi_i=\frac{2e}{\hbar}V_i\ , \tag{7}$$

where $\tilde{C}_{ii}=\sum_{j\neq i}C_{ij}$ and $\tilde{C}_{ij}=-C_{ij}$ for $i\neq j$. Equation (6) can be rewritten in matrix form:

$$\underline{\tilde{C}}\frac{d}{dt}\mathbf{V}=\mathbf{S}(\{V_i\},\{\phi_i\},t) \tag{8}$$

where $\mathbf{V}$ and $\mathbf{S}$ are the column vectors corresponding to the grain voltages $V_i(t)$ and the sums $S_i(t)$; $\underline{\tilde{C}}$ is the coupling capacitance matrix. (Note that in these calculations, we are neglecting the capacitive coupling between each grain and the ground.) For an $N\times N$ square plaquette array, $\underline{\tilde{C}}$ is an $(N^2+N)\times(N^2+N)$ order matrix. Hence, the matrix equation (8) consists of N^2+N equations in total. However, we can always set the phase of any one grain equal to an arbitrary constant (this is equivalent to grounding that grain), thereby reducing the number of independent phases and equations to N^2+N-1. If one equation is thus discarded from Eq. (8), the remaining matrix equation can be inverted to give

$$\frac{d}{dt}\mathbf{V}=\underline{\tilde{C}}^{-1}\mathbf{S}(\{V_i\},\{\phi_i\},t)\ . \tag{9}$$

We solve the coupled equations (7) and (9) by a straightforward Euler iteration, as described previously,[19] with time step Δt. Δt is usually chosen as $0.02t_0$, but occasionally as small as $0.01t_0$–$0.005t_0$, where $t_0=\hbar/(2eRI_c)$ is a characteristic damping time. A second-order Runge-Kutta method leads to little change in the results. In the calculations, we always start the iterations from zero applied external current. The initial phase of each grain is independently chosen from a uniform distribution of random numbers on $(0,2\pi)$, but the

initial voltage of each grain is set to zero, consistent with the likely experimental conditions. When increasing or decreasing the applied bias current, we use the final phase and voltage configurations of the array at the previous bias as the initial conditions for the new bias. To obtain time-average values, we usually discard results from the first time interval of $400t_0$, averaging over the next $800t_0$ (but occasionally over as long as $1000t_0-1200t_0$). In all the present calculations, we have taken the shunt capacitances, shunt resistances and critical currents to be the same for each junction, and equal to C, R, and I_c (corresponding to a homogeneous array). We characterize the array by the (dimensionless) junction McCumber-Stewart parameter,[18] which is defined by the relation $\beta=2R^2I_cC/\hbar$.

B. Choice of magnetic gauge

The effect of a transverse magnetic field **B** enters the equations of motion through the vector potential **A**, where

$$\oint_l \mathbf{A}\cdot d\mathbf{l}=\int\int_S \mathbf{B}\cdot d\mathbf{S}\ ,$$

S being the area of a plaquette of circumference l. In most calculations of this kind,[19,21] it is convenient to use the Landau gauge, $\mathbf{A}=Bx\hat{\mathbf{y}}$ for a uniform magnetic field $\mathbf{B}=B\hat{\mathbf{z}}$ in the direction perpendicular to the array. But for $f=\delta$ and $f=\frac{1}{2}+\delta$, with $|\delta|\ll 1$, the Landau gauge is not a convenient choice if one describes also to maintain periodic boundary conditions in the transverse directions. We therefore use a different gauge, previously employed by Arovas and Haldane in a different context.[22]

To define this gauge, we consider a square array a lattice constant a, with the origin taken as the lower left-hand corner of the array. Note that because of the periodic boundary conditions in the x direction, $x=Na$ is equivalent to $x=0$. Then A_{ij} is given by

$$A_{ij}=2\pi fn \tag{10}$$

for bonds in the y direction at $x=na$ $(0\le n\le N-1)$;

$$A_{ij}=0 \tag{11}$$

for all bonds in the x direction except for those in the extreme right-hand column of plaquettes; and

$$A_{ij}=-2\pi fNm \tag{12}$$

for bonds in the x direction in that extreme right-hand column, at $y=ma$. With this choice, the factors A_{ij} sum to $2\pi f$ around each plaquette, as required. Transverse periodicity will be satisfied as long as f is a multiple of $1/N^2$. This requirement is much weaker than that imposed by periodicity when the Landau gauge is used, which is that f be a multiple of $1/N$. Thus, the choice of gauge given by Eqs. (10)–(12) permits study of a much finer grid of flux densities than in previous studies.

III. RESULTS

A. $f=\delta$

Figure 1 shows the calculated I-V characteristics of an 8×8 array at $f=0$ for two different values of β. In each case, a random initial phase configuration and zero initial voltage configuration were chosen, as described in Sec. II. To generate the I-V characteristics, the applied current was ramped up in units of $0.005I_c$, starting from an initial value of zero. The time-averaged voltages were determined by averaging over a time interval of $800t_0$ after discarding the first $400t_0$ of voltages. The curves show that the array behaves much like a single junction, as has been observed previously,[19] with a sharp critical current at $I=I_c$. In the overdamped limit ($\beta=0$), for currents greater than the critical current I_c, the voltage rises proportionally to $\sqrt{I-I_c}$, consistent with analytical results

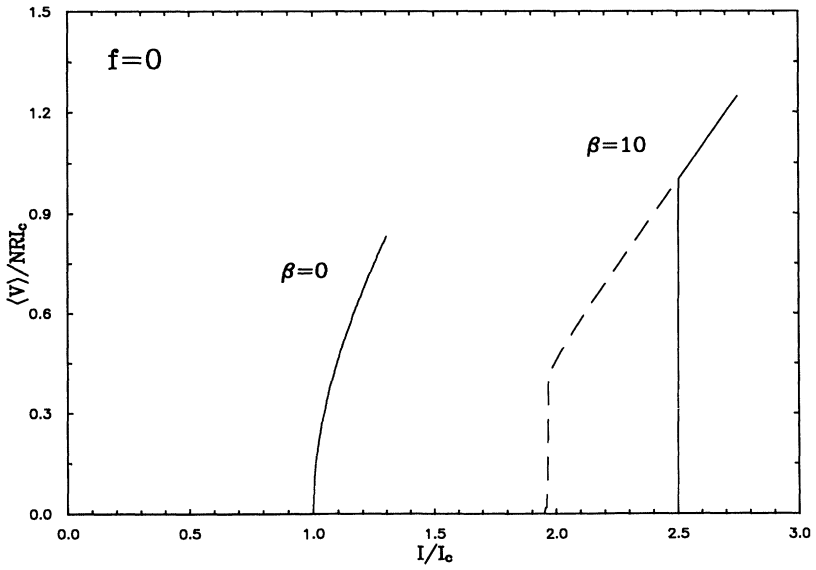

FIG. 1. I-$\langle V\rangle$ characteristics of an 8×8 array with periodic boundary conditions at $f=0$ and two values of the McCumber-Stewart parameter β. In this and subsequent figures, the solid curves are obtained with increasing applied current, the dashed curves with decreasing current. The origin of the $\beta=10$ curve is offset to the right by 1.5 units.

for a single overdamped Josephson junction. At larger values of β, we find that the transition into the resistive state at the critical current I_c becomes steeper and steeper, and at sufficiently large values of β, there is clear hysteresis in the I-V characteristics, just as in single junctions of similar β values.[18] This hysteresis is clearly visible at $\beta=10$.

In a single junction, this hysteresis is due to the mass of a phase "particle" sliding down a washboard potential. For a sufficiently underdamped particle, this sliding motion (i.e., a finite voltage) is maintained even when the slope of the washboard potential (i.e., the current) is decreased far below its critical value for onset of the motion. The hysteresis seen in Fig. 1 is simply this same behavior for a locked array of Josephson junctions.

Figure 2 is the analog of Fig. 1 at $f=\frac{1}{64}$. The curves are similar to those at $f=0$ except for a low-current voltage tail, corresponding to the motion of a single vortex. In addition, the I-V characteristic has an apparent slope discontinuity near $I=I_c$. These curves reveal *two* critical currents, $I_{c1}(f=0)$ and $I_{c2}(f=0)$. $I_{c1}(0)\approx 0.11 I_c$ for any value of β, and represents the current necessary to depin a single vortex. This value agrees with the static predictions of Ref. 3. $I_{c2}(0)$ is very nearly equal to I_c, the critical current at $f=0$, and correspond to the depinning of the ground-state phase configuration of the entire lattice, as in Fig. 1.

At sufficiently large β, there are usually one or more discontinuities in the I-V curve as the current is increased. These are due to row switching.[5–8] When the vortex (depinned at a current of $\approx 0.11 I_c$) acquires sufficient kinetic energy, it loses that kinetic energy to a row of junctions perpendicular to the direction of the current (i.e., parallel to the direction of vortex motion; see Fig. 3). All the junctions in that row are switched into a resistive state, giving rise to the resistance step seen in Fig. 2. This behavior has been seen experimentally,[5,6] and also reported in previous simulations.[19] Note that

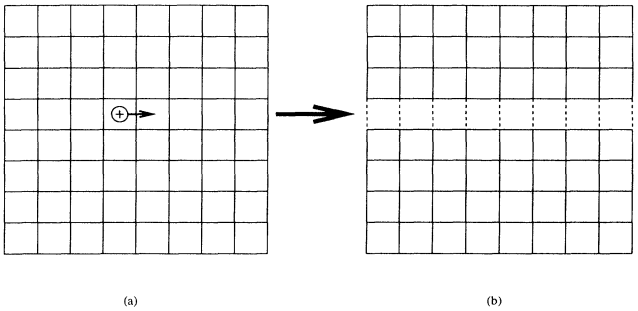

FIG. 3. schematic illustration of row-switching behavior in a current-drive Josephson-junction array containing a single vortex. (a) A single vortex (denoted by a circled + sign) moves perpendicular to the applied current. (b) At sufficiently high current, the vortex breaks up into a row of resistively switched junctions (dashed lines parallel to the current), leading to a step increase in the array resistance.

the row switching occurs at lower values of current as β is increased. This is presumably because, for a given current, the moving vortex has a larger kinetic energy at larger values of β and hence can more easily trigger the row switching. When the current is increased above $I_{c2}(f=\frac{1}{64})$ and then reduced, the array shows conspicuous hysteresis at large values of β, just as it does for $f=0$.

Figure 4 shows the time-dependent voltage traces $V(t)$ at $f=\frac{1}{64}$ for two representative current levels at $\beta=0$. Just above the critical current of about $I_{c1}(0)=0.11 I_c$, $V(t)$ looks like that of a *single* Josephson junction: there are a series of voltage spikes [Fig. 4(a)]. The frequency of these spikes increases with increasing voltage. In general, the period $T\equiv 1/\nu$ of these spikes is related to the time-averaged voltage $\langle V\rangle$ across the array by $\langle V\rangle=(h\nu/2eN)$ in an $N\times N$ array. This corresponds to the motion of a single vortex perpendicular to the

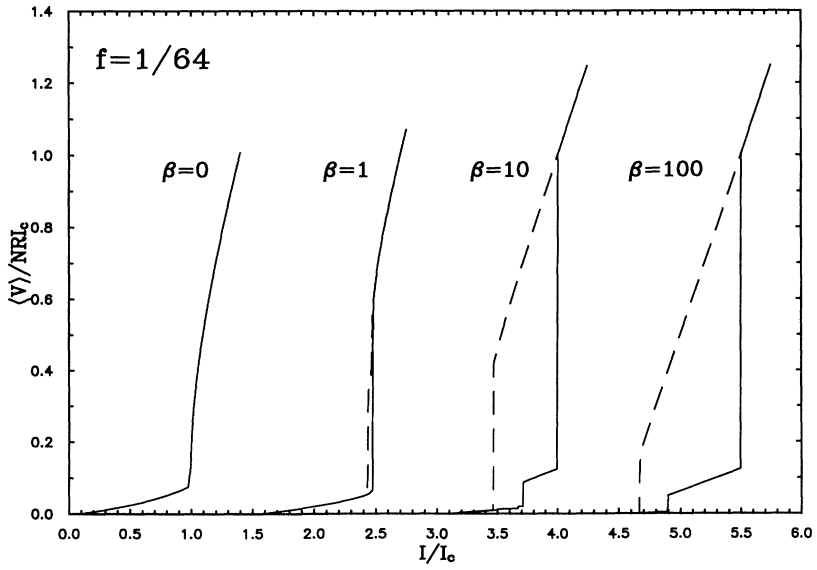

FIG. 2. Same as Fig. 1, but for $f=\frac{1}{64}$ and four values of β. The origin of successive β curves is offset to the right by 1.5 units.

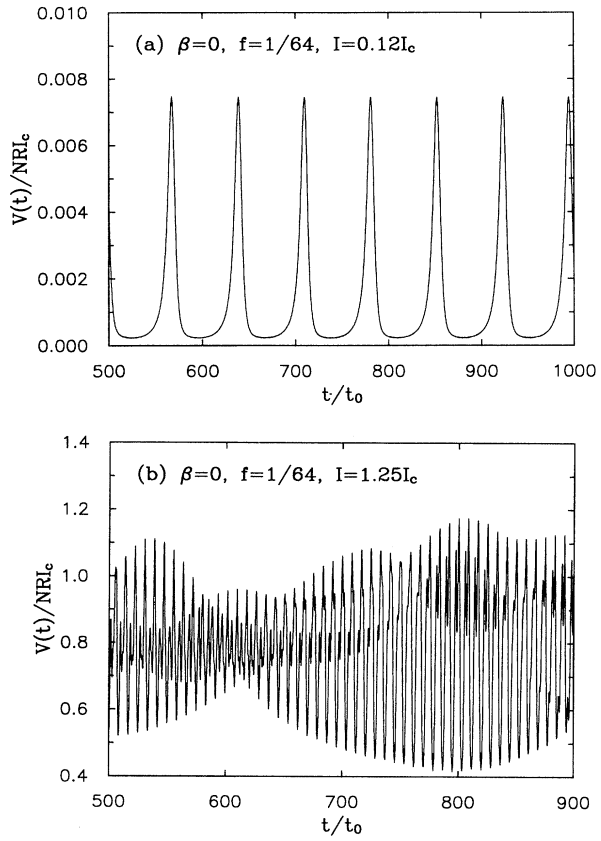

FIG. 4. Time-dependent voltage traces for $f=\frac{1}{64}$ and two values of the applied current I. In both cases, $\beta=0$. t_0 denotes the time scale, $t_0=\hbar/(2eRI_c)$.

current, through the periodic two-dimensional potential formed by the array, by a distance of a plaquette in a period T. Thus, there is a phase slip of 2π in a time NT, associated with the motion of a vortex across the entire array. For $I>I_c$, the voltage is aperiodic in general, but at sufficiently large currents [e.g., $I_{\rm ext}=1.25I_c$; Fig. 4(b)] $V(t)$ is a periodic function modulated by a very low-frequency envelope. The frequency ν of the rapid oscillations is now related to the time-averaged voltage by $\langle V\rangle \approx Nh\nu/(2e)$. Each period $T=1/\nu$ now corresponds to a phase slip of 2π by every junction parallel to I, i.e., the entire ground-state lattice is depinned at these currents.

The vortex equation (1) suggests that the I-V curves will be hysteretic at sufficiently large values of β. But since I_d is much smaller than I_c, the effective β for the array will be reduced by about a factor of I_d/I_c relative to a single junction. Hence, much larger values of β should be needed to see hysteresis in an array. This is confirmed in Fig. 5, which shows the calculated I-V curves for an 8×8 array at $f=\frac{1}{64}$ at $\beta=10$. This figure actually shows two curves, for increasing and decreasing current, which are virtually indistinguishable. The curves were generated starting from a random initial phase configuration and zero initial voltages. The applied current was ramped up in units of $0.002I_c$ from zero initial value to $0.25I_c$ for the $\beta=10$ curve [well below the upper critical current $I_{c2}(0)$ described above], then ramped down in the same steps to zero. $\langle V\rangle$ was calculated by averaging over a time interval of $1000t_0$ after discarding the voltages over the first interval of $1000t_0$. Evidently, there is almost *no* hysteresis even at $\beta=10$, even though a *single* underdamped Josephson junction of this β would be highly hysteretic. At $\beta=100$ (not shown) we saw some signs of hysteresis. Thus, a vortex moving in an array of highly underdamped junctions seems to behave as if it were an overdamped object. Although counterintuitive, this result seems to be consistent with experiment[6] as well as with Eq. (1).

B. $f=\frac{1}{2}+\delta$

Figure 6 shows results analogous to Figs. 1 and 2 at fields $f=\frac{1}{2}$ and $f=\frac{33}{64}$. The I-V characteristics at $f=\frac{1}{2}$

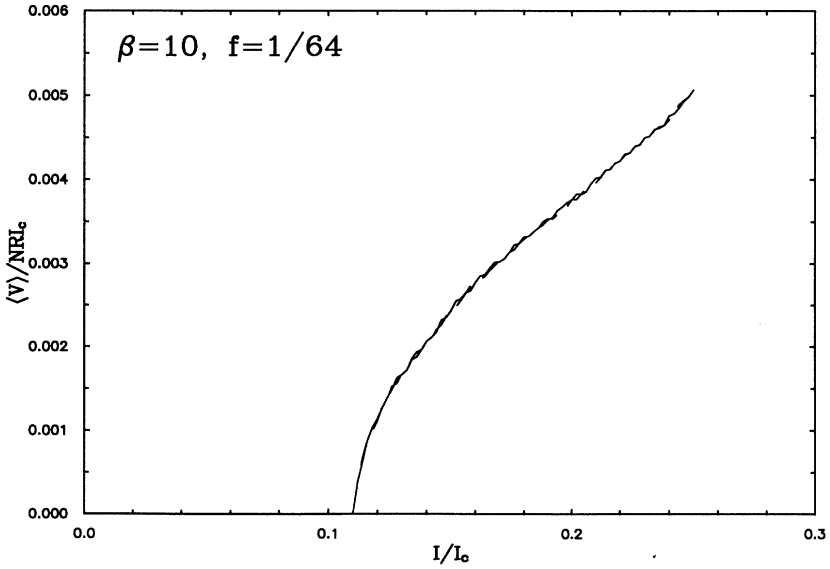

FIG. 5. I-$\langle V\rangle$ characteristics of an 8×8 array with periodic boundary conditions at $f=\frac{1}{64}$, and $\beta=10$. In contrast to Fig. 2, the current is increased only up to $I=0.25I_c$, well below the upper critical current $I_{c2}(0)$. Shown are curves for increasing current and decreasing current, which nearly coincide for this value of β, indicating no hysteresis.

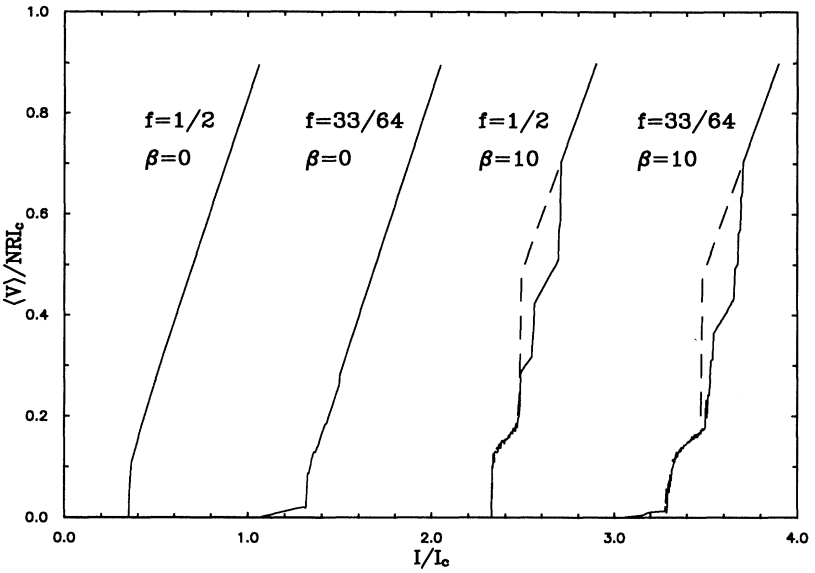

FIG. 6. Same as Fig. 1 but for $f=\frac{1}{2}$ and $f=\frac{33}{64}$ and two values of β. Successive curves for different parameters are offset to the right by one unit.

exhibit a critical current $I_{c2}(1/2)\approx 0.35I_c$, somewhat reduced at the highest value of β. At $f=\frac{33}{64}$, the I-V characteristic has a low-current tail with critical current $I_{c1}(1/2)\approx 0.1I_c$, corresponding to the motion of a single vortexlike excitation in the background of the $f=\frac{1}{2}$ ground-state phase configuration. Near $I_{c2}(\frac{1}{2})$, the I-V characteristic shows an abrupt change of slope. Above $I_{c2}(\frac{1}{2})$, the entire $f=\frac{1}{2}$ ground state is depinned, giving rise to a much larger voltage.

Figure 6 also show how hysteresis develops near $f=\frac{1}{2}$ as β increases. For both $f=\frac{1}{2}$ and $f=\frac{33}{64}$, the arrays show little hysteresis at small β, but much more at $\beta=10$. The nonhysteretic behavior at low β presumably arises as a uniform translation of the $f=\frac{1}{2}$ ground-state vortex lattice perpendicular to the current. At large β, this lattice has such a high kinetic energy density that it can generate row-switching behavior, similar to what is seen at $f=\frac{1}{64}$. At $\beta=100$, which we do not show in the figures, we find that the $f=\frac{1}{2}$ vortex lattice apparently has no region of dynamic stability: no sooner is it depinned than it generates a row-switching event. As the current is further increased, for these large β's, there are additional row switchings. These rows remain in a resistive state as the current is decreased, leading to hysteretic I-V characteristics. The same kind of row switching occurs at $f=\frac{33}{64}$. At $\beta=10$, only the moving $f=\frac{1}{2}$ lattice seems to have enough kinetic energy to generate row switches; none are produced by individual vortexlike excitations superimposed on this lattice. For $\beta=100$, these excitations may suffice to produce row switching even at lower current densities.

To shed further light on the motion of single vortices near $f=\frac{1}{2}$, we have also computed the time-dependent voltages across the array at several current levels for $f=\frac{33}{64}$. In the single vortex region [roughly $I\le I_{c2}(\frac{1}{2})\equiv 0.35I_c$], the motion depends on the initial phase configuration, i.e, on the initial position of the vortex. Other initial conditions can lead to quite different $V(t)$'s. Figure 7 shows some representative results, for one particular choice of (random) initial phases at $\beta=0$ and $f=\frac{33}{64}$. The vortex moves in a periodic orbit through

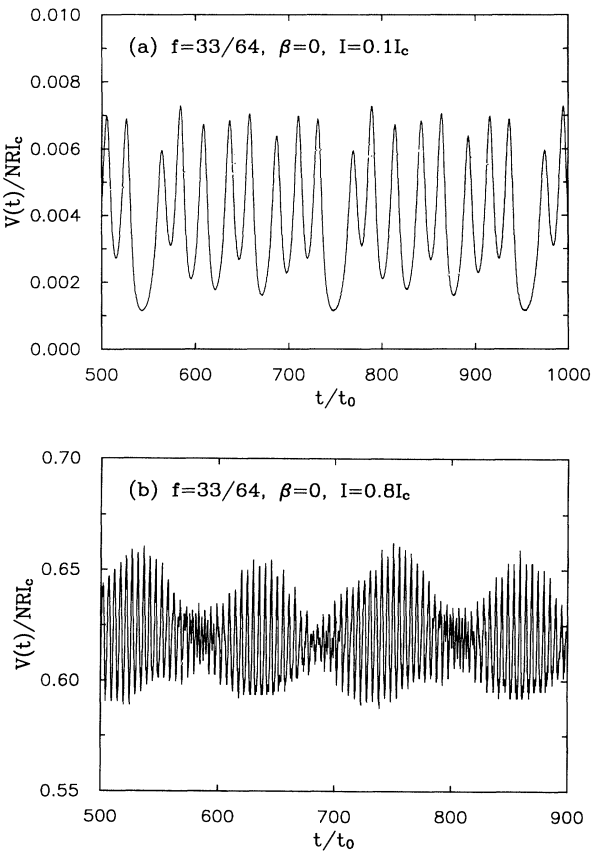

FIG. 7. Time-dependent voltage traces for $f=\frac{33}{64}$, $\beta=0$, and two values of the applied current I.

the 8×8 array (which has periodic transverse boundary conditions), as can be inferred from the fact that $V(t)$ is periodic in time [Fig. 7(a)]. Every period has eight voltage peaks of unequal height, each peak corresponding to a transverse motion of the vortex by one plaquette. With increasing current, the vortex moves more and more rapidly through the background of the $f=\frac{1}{2}$ ground state. Just below $I=I_{c2}(\frac{1}{2})\approx0.35I_c$, $V(t)$ is a series of small oscillations occasionally disturbed by a broad but intense voltage pulse (not shown). We interpret the small oscillations as single vortex motions, the large aperiodic pulses as translations of the entire underlying $f=\frac{1}{2}$ lattice. At still higher currents $V(t)$ is a nearly periodic function modulated, as at $f=\frac{1}{64}$, by a slowly varying envelope [Fig. 7(b)]. Each rapid oscillation of $V(t)$ now corresponds to a translation of the entire underlying $f=\frac{1}{2}$ ground-state phase configuration by one plaquette. This interpretation can be verified by relating the voltage to the period T of the modulated oscillations, as shown in Fig. 7. To a good approximation, $\langle V\rangle\approx(8/T)2\pi(\hbar/2e)(\frac{1}{2})$. This corresponds to a phase slip of 2π for each junction parallel to the current in every interval $2T$, as would be expected for an $f=\frac{1}{2}$ ground-state phase configuration moving perpendicular to the current.

Figure 8 summarizes our qualitative picture of the I-V characteristics at both $f=\delta$ and $f=\frac{1}{2}+\delta$. In the former case, there is a single isolated positive vortex (denoted by a plus sign) moving in an otherwise empty periodic two-dimensional lattice. There are correspondingly two critical currents, $I_{c1}(0)$ and $I_{c2}(0)$ representing the depinning of the individual vortices and the entire array of phase differences. At $f=\frac{1}{2}+\delta$, there is an extra vortex in the checkerboard $f=\frac{1}{2}$ ground state. The I-V characteristic again exhibits two critical currents, $I_{c1}(\frac{1}{2})$ and $I_{c2}(\frac{1}{2})$. The first leads to motion of a single vortex through the checkerboard background. Above $I_{c2}(\frac{1}{2})$, the checkerboard background itself is depinned and moves perpendicular to the current, giving rise to nearly periodic voltage spikes.

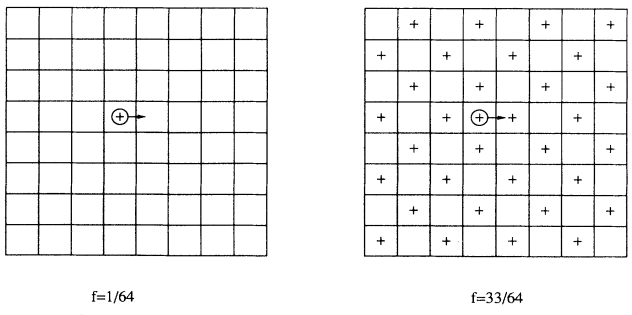

FIG. 8. Schematic of the vortex pattern and the expected I-V characteristics at $f=\delta$ and $f=\frac{1}{2}+\delta$. The schematic corresponds to $\delta=\frac{1}{64}$ in an 8×8 lattice. Plus signs denote positive vortices, empty squares denote absence of positive vortices. The circled vortex moves in the direction shown under an applied current I (introduced from below) which exceeds the vortex depinning current I_{c1}.

We have checked for hysteresis when a single vortex moves in an $f=\frac{1}{2}$ background. So long as the current is never increased above $I_{c2}(\frac{1}{2})$, the I-V characteristics are apparently nonhysteretic, even for $\beta\gg10$. In this respect, the vortex motion at $f=\frac{1}{2}+\delta$ is similar to that at $f=\delta$.

IV. DISCUSSION

Our results regarding the coherent motion of vortices have a number of implications for real experiments. One striking result is the finite critical currents we find at $f=\delta$ and at $f=\frac{1}{2}+\delta$. These finite critical currents imply a finite vortex depinning *energy* $E_d(f)$ for a vortex in a lattice at $f=0$ and $f=\frac{1}{2}$, as has already noted by a number of workers.[2,3] A finite depinning energy may lead, in turn, to an activated low-temperature resistivity[4,12] of the form $|\delta|\exp[-E_d(f)/k_BT]$, in a regime where the excited vortices behave as independent diffusing particles.

We can also extrapolate our results to other values of f. By extension from $f=0$ and $f=\frac{1}{2}$, we may assume that the defect vortices at other f's will move through a still more complex "partially filled periodic two-dimensional" potential formed by the underlying vortex lattice. For example, at $f=\frac{1}{3}$, one-third of the possible plaquettes are filled by vortices. On the basis of the ground state proposed in Ref. 20 for this state, we might expect that a vortex defect traveling parallel to one of the axes of the square lattice would move through a potential in which one-third of the plaquette centers correspond to potential maxima, while the other two-thirds represent minima. This potential, unlike that at $f=\frac{1}{2}$, would *not* be symmetric with respect to $\delta=0$, and should be characterized by still more complex time-dependent vortex motions.

A surprise in our calculations (as well as experiment) is the absence of hysteresis in vortex motion even at large values of β for both $f=\delta$ and $f=\frac{1}{2}+\delta$. Seemingly, a vortex behaves like an overdamped object even in an array of highly underdamped junctions.

In an effort to further understand this overdamped behavior, we have ramped the current up to $0.25I_c$ at $f=\frac{1}{64}$ and various values of β, then *abruptly turned off the current.* In all cases up to $\beta=1000$, the vortex oscillates with exponentially decreasing amplitude about its initial position at the time the current is turned off. This behavior is indicated by exponentially decaying voltage oscillations. Clearly, the initial kinetic energy reached at $I=0.25I_c$ is too small to allow ballistic vortex motion when the current is removed. Hence, in order to produce ballistic motion at *any* β, one would need to inject vortices initially with some *large* kinetic energy. When the current is ramped up to $0.9I_c$ at $\beta=1000$, then turned off, one obtains the voltage trace shown in Fig. 9, which looks like the signature of a moving vortex which gradually slows and is eventually trapped. This interpretation is probably not correct, however. Instead, the trace represents the time decay of the two switched rows which are generated under these conditions. While ballistic vortex motion doubtless exists under proper initial condi-

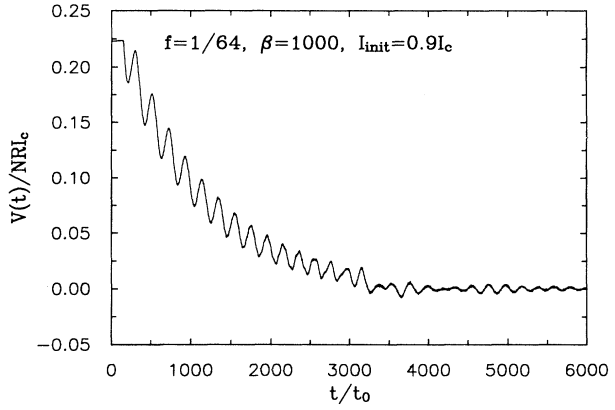

FIG. 9. Voltage trace $V(t)$ in an 8×8 array at $f=\frac{1}{64}$, $\beta=1000$, after the current is ramped up to $I=0.9I_c$ and abruptly removed. The voltage trace represents, not the slowing down and retrapping of a vortex, but the decay of the two switched rows which already exist in this array at time $t=0$.

tions, we have not as yet seen it in our calculations.

On the basis of these simulations, we tentatively conclude that, in very underdamped arrays, vortices with high kinetic energy tend to decay by row switching rather than to move ballistically. Lower-energy vortices move coherently but have insufficient kinetic energy to propagate ballistically, i.e., to continue moving when the driving current is turned off, and hence, the corresponding I-V characteristics do not show any hysteresis.

In Refs. 5 and 6, it is suggested that the vortices in an underdamped array still move in an overdamped fashion because they lose energy to single junctions oscillating in their wakes at the Josephson plasma frequency. This picture is not inconsistent with our own results. However, we have not investigated the voltage oscillations of single junctions in the wakes of moving vortices, and so have not explicitly confirmed this picture.

Note that all the calculations presented here are for an 8×8 array. We expect that some of our results may well be size dependent (e.g., the current at which a vortex decays into a resistively switched row), but have not as yet investigated this size dependence. Since our depinning currents, at least for $f=\frac{1}{64}$, are close to those calculated form much larger lattices,[2,3] it seems likely that most size effects will not be too severe.

To conclude, we have calculated single vortex motion in both underdamped and overdamped Josephson-junction arrays at fields $f=\delta$ and $f=\frac{1}{2}+\delta$. In both cases, we see clear evidence for coherent vortex motion on the background of the ground-state phase configuration, with characteristic activation energies. The vortices tend to behave in an overdamped (i.e., nonhysteretic) fashion even if the junctions themselves are underdamped, in agreement with experiment. The calculations also show that the vortices can generate resistance steps at sufficiently large β, once again in agreement with measurements on underdamped arrays. We suggest some possible explanations for the nonhysteretic vortex behavior, and discuss how ballistic vortex motion might be produced.

ACKNOWLEDGMENTS

We should like to thank Professor S. M. Girvin for calling our attention to the gauge that made these calculations feasible, and Professor D. P. Arovas for a useful discussion. This work was supported by National Science Foundation through Grant No. DMR 90-20994, and by the Midwest Superconductivity Consortium through DOE Grant No. DE-FG02-90ER45427. Calculations were carried out, in part, on the CRAY Y-MP 8/864 of the Ohio Supercomputer Center, with the help of a grant of time which we gratefully acknowledge.

[1]For many references up to 1988, see, e.g., the articles in Physica (Amsterdam) **152B**, pp. 1–302 (1988).

[2]M. S. Rzchowski, S. P. Benz, M. Tinkham, and C. J. Lobb, Phys. Rev. B **42**, 2041 (1990).

[3]C. J. Lobb, D. W. Abraham, and M. Tinkham, Phys. Rev. B **27**, 150 (1983).

[4]H. S. J. van der Zant, F. C. Fritschy, T. P. Orlando, and J. E. Mooij, Physica B **165-66**, 969 (1990).

[5]H. S. J. van der Zant, F. C. Fritschy, T. P. Orlando, and J. E. Mooij, Phys. Rev. Lett. **66**, 2531 (1991).

[6]T. S. Tighe, A. T. Johnson, and M. Tinkham, Phys. Rev. B **44**, 10286 (1991).

[7]H. S. J. van der Zant, C. J. Muller, L. J. Geerligs, C. J. P. M. Harmans, and J. E. Mooij, Phys. Rev. B **38**, 5154 (1988).

[8]H. S. J. van der Zant, H. A. Rijken, and J. E. Mooij, J. Low. Temp. Phys. **79**, 289 (1990); **82**, 67 (1991).

[9]R. A. Webb, R. F. Voss, G. Grinstein, and P. M. Horn, Phys. Rev. Lett. **51**, 690 (1983).

[10]For recent discussions of the influence of charging energy, see, e.g., Rosario Fazio and Gerd Schön, Phys. Rev. B **43**, 5307 (1991), and references cited therein.

[11]Some representative experimental references on overdamped Josephson arrays include D. J. Resnick, J. C. Garland, J. T. Boyd, S. Shoemaker, and R. S. Newrock, Phys. Rev. Lett. **47**, 1542 (1981); M. Tinkham, D. W. Abraham, and C. J. Lobb, Phys. Rev. B **26**, 6578 (1983); Ch. Leeman, P. Lerch, G. A. Racine, and P. Martinoli, Phys. Rev. Lett. **56**, 1291 (1986); D. Kimhi, F. Leyvraz, and D. Ariosa, Phys. Rev. B **29**, 1487 (1984).

[12]Y. M. Ivanchenko and L. A. Zil'berman, Zh. Eksp. Teor. Fiz. **55**, 2395 (1968) [Sov. Phys. JETP **28**, 1272 (1969)].

[13]A. I. Larkin, Yu. N. Ovchinnikov, and A. Schmid, Physica (Amsterdam) **152B**, 266 (1988); S. E. Korshunov, *ibid.* **152B**, 261 (1988).

[14]U. Eckern and A. Schmid, Phys. Rev. B **39**, 6441 (1989).

[15]M. P. A. Fisher, Phys. Rev. Lett. **65**, 923 (1990).

[16]S. P. Benz, M. S. Rzhhowski, M. Tinkham, and C. J. Lobb, Phys. Rev. Lett. **64**, 693 (1990).

[17]K. H. Lee, D. Stroud, and J. S. Chung, in *Proceedings of the NATO Advanced Studies Workshop on Relaxation and Related Phenomena in Glassy Systems*, edited by I. Campbell and C. Giovannella (Plenum, New York, 1990), pp. 623-630.

[18]W. C. Stewart, Appl. Phys. Lett. **22**, 277 (1968); D. E. McCumber, J. Appl. Phys. **39**, 3113 (1968).

[19]Wenbin Yu and D. Stroud, Phys. Rev. B **46**, 14 005 (1992).

[20]S. Teitel and C. Jayaprakash, Phys. Rev. B **27**, 598 (1983); S. Teitel and C. Jayaprakash, Phys. Rev. Lett. **51**, 1999 (1983).

[21]Some representative recent dynamical calculations on Josephson-junction arrays (all for overdamped arrays, unless otherwise indicated) include K. K. Mon and S. Teitel, Phys. Rev. Lett. **62**, 673 (1989); A. Falo, A. R. Bishop, and P. S. Lomdahl, Phys. Rev. B **41**, 10 983 (1990); T. C. Halsey, *ibid.* **41**, 11 634 (1990); W. Xia and P. L. Leath, Phys. Rev. Lett. **63**, 1428 (1989); H. Eikmans and J. E. van Himbergen, Phys. Rev. B **41**, 8927 (1990); L. I. Sohn, M. S. Rzchowski, J. U. Free, S. P. Benz, M. Tinkham, and C. J. Lobb, *ibid.* **44**, 925 (1991); D. Domínguez, J. V. José, A. Karma, and C. Wiecko, Phys. Rev. Lett. **67**, 2367 (1991); K. H. Lee, D. Stroud, and J. S. Chung, *ibid.* **64**, 962 (1990); M. Octavio, J. U. Free, S. P. Benz, R. S. Newrock, D. B. Mast, and C. J. Lobb, Phys. Rev. B **44**, 4601 (1991); K. Y. Stang, S. H. Strogatz, and K. Wiesenfeld, Phys. Rev. Lett. **66**, 1094 (1991); R. Bhagavatula, C. Ebner, and C. Jayaprakash, Phys. Rev. B **45**, 4774 (1992) (underdamped arrays).

[22]D. P. Arovas and F. D. M. Haldane (unpublished).